Dyes and Pigments 191 (2021) 109382

Contents lists available at ScienceDirect

Dyes and Pigments

journal homepage: http://www.elsevier.com/locate/dyepig

Design of flexible dendritic systems bearing donor-acceptor groups (pyrene-porphyrin) for FRET applications

Yoliztli Bañales-Leal [a], Andrea García-Rodríguez [a], Fabián Cuétara-Guadarrama [a], Mireille Vonlanthen [a], Kendra Sorroza-Martínez [a], David Morales-Morales [b], Ernesto Rivera [a,*]

[a] Instituto de Investigaciones en Materiales, Universidad Nacional Autónoma de México, Circuito Exterior, Ciudad Universitaria, Mexico City, CP 04510, Mexico
[b] Instituto de Química, Universidad Nacional Autónoma de México, Circuito Exterior, Ciudad Universitaria, Mexico City, CP 04510, Mexico

ARTICLE INFO

Keywords:
Energy transfer (FRET)
Optical properties
Dendrimer
Pyrene
Porphyrin

ABSTRACT

Herein, we report the synthesis and characterization of a novel series of dendritic compounds, bearing peripheral pyrene groups and a porphyrin core, of zero and first generation with different spacer lengths. These compounds were further metallated with Zn(II) and Mg(II). The optical properties of these dendritic molecules were studied by absorption and fluorescence spectroscopy. After metallation, the dendritic porphyrins exhibited a red shift in the Soret absorption band and a blue shift in the emission band. All compounds exhibited high energy transfer efficiency, reaching values of E_{FRET} above 99%.

1. Introduction

In the last decades dendritic molecules have attracted much attention, being motif of multiple studies to investigate their outstanding physical and chemical properties [1–4]. Hence, dendrimers and dendrons are promising compounds for the elaboration of electroactive and photoactive devices, for their biological applications in the administration and controlled drug delivery, as well as for their potential use as catalysts for organic transformations [5–11]. Moreover, the photophysical properties of photoactive dendrimers can be finely tuned by the careful design of their architectures, allowing the location of the photoactive units either in the core, in the dendritic building units or at the periphery. This permit the observation of fluorescence resonance energy transfer (FRET) and charge transfer (CT), photophysical phenomena that are very important in the development of photovoltaic devices [12–16].

In this sense, and due to its unique and outstanding optical and photophysical properties, pyrene has been widely used as fluorescent probe in various dendritic and polymeric structures [17–20]. It is worth mentioning that this chromophore can produce either inter or intramolecular excimers, by increasing its local concentration or by interacting with another pyrene unit present in the same molecule, respectively [21–23]. Thus, dendritic and polymeric architectures bearing pyrene, covalently linked to diverse acceptor groups have been reported [24–27].

In addition, the porphyrin chromophore motif has been widely applied in photodynamic therapy, catalysis, non-linear optics, fluorescent switches, etc [28–32]. One of the most notable applications of porphyrins, has been their incorporation as acceptor in many dendritic structures, as part of the design of solar cells based on photosynthesis mimicking molecular systems (acting as sensitizers of light absorption) [33–35]. Hence, a large number of dendritic structures with donor-acceptor groups having porphyrin chromophores has been reported [36,37]. Some important contributions from our research group have been reported on the study of dendritic structures based on the pyrene-porphyrin donor-acceptor pair for energy transfer purposes, leading to energy transfer efficiencies close to 100% [38–43].

Furthermore, important biological porphyrin derivatives for dioxygen transport and photosynthesis are based on metalloporphyrins. Some relevant examples are the iron, magnesium and cobalt complexes found in the heme, chlorophyll and vitamin B_{12}, respectively [44–47]. In addition, artificial metalloporphyrin complexes such as meso substituted porphyrins can be synthesized and modified in a facile manner. The two main features of these systems are the appearance of a strong absorption band in the blue region of the UV–vis spectrum (Soret band), and low intensity Q bands near the red region [48,49]. The coordination of the porphyrin with a metal ion provokes changes in the observed absorption spectra, therefore changing the photophysical and redox properties [50,51]. Metalloporphyrins have been used in analytical chemistry, catalysis (*i.e.* oxidation reactions) and as building blocks

* Corresponding author.
E-mail address: riverage@unam.mx (E. Rivera).

https://doi.org/10.1016/j.dyepig.2021.109382
Received 6 October 2020; Received in revised form 22 February 2021; Accepted 6 April 2021
Available online 17 April 2021
0143-7208/© 2021 Elsevier Ltd. All rights reserved.

for the production of metal organic frameworks (MOF's) [52–57].

We have previously studied the effect of metallation (Zn, Cu, Mg, and Mn) of some pyrene-labeled dendronized porphyrins on their energy transfer from the pyrene moiety [41]. The UV–vis and fluorescence properties of the series of compounds have been studied and these systems include Fréchet type rigid dendrons. Therefore, in this work we have performed the synthesis of a new series of pyrene dendronized porphyrins of zero and first generations. These Newkome type dendrimers bear a flexible structure with the aim of facilitating the further encounter of the pyrene-porphyrin donor-acceptor pair [58,59].

2. Experimental part

2.1. General notes

All the reagents employed in the synthesis were purchased from Merck Sigma Aldrich and used as received. The solvents used in the reactions were purified by simple distillation in the presence of a drying agent (CaH_2 for dichloromethane). The products were purified by column chromatography in silica gel and the composition of the eluting solvent was selected after thin layer chromatography (TLC) experiments. All compounds were characterized by ^1H and ^{13}C NMR spectroscopy in $CDCl_3$. NMR spectra were recorded on a Bruker Avance 400 MHz, working at 400 MHz and 100 MHz for ^1H and ^{13}C, respectively. Chemical shifts are reported in parts per million. Multiplicity is given as s (singlet), d (doublet), t (triplet), q (quadruplet), quint (quintuplet) or m (multiplet). MALDI-TOF mass spectra were recorded on a Bruker Daltonics Flex Analysis employing dithranol as matrix. FAB analyses were recorded on an MStation JMS-700 instrument. Elemental analyses were performed in a Thermo Scientific Flash 2000 elemental analyzer, using a Mettler Toledo XP6 Automated-S Microbalance and sulfanilamide as standard (Thermo Scientific BN 217826, attained values N = 16.40%, C = 41.91%, H = 4.65%, and S = 18.63%; certified values N = 16.26%, C = 41.81%, H = 4.71%, y S = 18.62%). Absorption spectra were recorded on a Unicam UV300 spectrophotometer using quartz cells with a width of 1 cm and THF (spectrometric grade) as solvent. Fluorescence spectra were carried out on a Horiba Fluorolog 3 spectrophotometer with a Xenon lamp. The slit width for excitation and emission were set up to 1 nm in both cases.

2.2. Synthesis of the dendritic porphyrin core

2.2.1. Synthesis of ethyl-4-(4-formylphenoxy) butanoate (1)

Compound **1** was synthesized according to the literature [60]. A mixture of 4-hydroxybenzaldehyde (1.00 g, 8.3 mmol) and K_2CO_3, (1.40 g, 9.6 mmol) was dissolved in anhydrous DMF (5 mL). Then, ethyl 4-bromobutyrate (1.90 g, 9.6 mmol) was added dropwise. The mixture was heated to 100 °C for 5 h. The solvent was removed under reduced pressure, and the crude was redissolved in CH_2Cl_2 (30 mL) and washed with distilled water (3 x 20 mL). The crude product was dried with Na_2SO_4, the solution filtrated, and the solvent removed under reduced pressure. The product was purified by column chromatography using a mixture hexanes/ethyl acetate 7:3 as eluent. The pure product **1** was obtained as a yellow liquid (1.63 g, 92%). ^1H NMR (δ ppm, 400 MHz, $CDCl_3$): 9.86 (s, 1H), 7.83 (d, 2H, J = 8.7 Hz), 6.99 (d, 2H, J = 8.7 Hz), 4.13 (q, 2H, J = 7.1 Hz), 4.10 (t, 2H, J = 6.2 Hz), 2.53 (t, 2H, J = 7.2 Hz), 2.15 (quint, 2H, J = 6.7 Hz), 1.26 (t, 3H, J = 7.1 Hz). ^{13}C NMR (δ ppm, 100 MHz, $CDCl_3$): 190.9 (CHO), 173.1 (CO), 164.0 (C), 132.1 (CH), 130.1 (C), 114.8 (CH), 67.2 (CH_2), 60.6 (CH_2), 30.7 (CH_2), 24.5 (CH_2), 14.3 (CH_3). Elemental Anal. Calcd (%) for $C_{13}H_{16}O_4$: C, 66.09; H, 6.83. Found: C, 66.05; H, 6.85.

2.2.2. Synthesis of porphyrin 2

A volume of 600 mL of anhydrous CH_2Cl_2 was poured into a round bottom flask under inert atmosphere and protected from light. Then, compound **1** (1.50 g 13.5 mmol), pyrrole (1.76 mL, 25.5 mmol), benzaldehyde (1.94 mL, 19.0 mmol), benzyltributylammonium chloride (BTBAC) (12.3 mg, 0.039 mmol) were mixed and some drops of EtOH were added and the mixture was stirred for 15 min. After this time, borontrifluoride diethyl etherate ($BF_3 \cdot OEt$) (0.32 mL, 2.5 mmol) was added and the mixture was further stirred for 15 min. Finally, 2,3-dichloro-5,6-dicyano-1,4-benzoquinone (DDQ) (4.33 g, 19 mmol) was added and the reaction was allowed to continue for 2 h. Trimethylamine (5 mL) was added to quench the reaction. The crude product was purified by column chromatography (neutral alumina), using a mixture of hexanes/CH_2Cl_2 as eluent, increasing gradually the polarity until hexanes/CH_2Cl_2 7:3 was reached. The desired product **2** was obtained as a purple solid (0.65 g, 14%). ^1H NMR (δ ppm, 400 MHz, $CDCl_3$): 8.91–8.86 (m, 8H), 8.31–8.17 (m, 6H), 8.12 (d, J = 8.6 Hz, 2H), 7.80–7.72 (m, 9H), 7.28 (d, J = 8.7 Hz, 2H), 4.30 (t, J = 6.2 Hz, 2H), 4.24 (q, J = 7.2 Hz, 2H), 2.70 (t, J = 7.1 Hz, 2H), 2.31 (quint, J = 6.5 Hz, 2H), 1.35 (t, J = 7.1 Hz, 3H), −2.79 (s, 2H). ^{13}C NMR (δ ppm, 100 MHz, $CDCl_3$): 190.9 (CHO), 142.3 (C2, C–NH), 135.8 (C3), 134.9 (C4, phenol), 129.2 (C5, phenyl groups), 127.8 (C6, phenyl groups), 126.8 (C7, C-meso-porphyrin), 120.1 (C8, phenol), 113.8 (C9, C- endo-porphyrin). MALDI-TOF: m/z calculated for $C_{50}H_{40}N_4O_3$ $[M]^+$: 744.31 found $[M]^+$: 744.51. Elemental Anal. Calcd (%) for $C_{50}H_{40}N_4O_3$: C, 80.62; H, 5.41; N, 7.52. Found: C, 80.66; H, 5.38; N, 7.47.

2.2.3. Synthesis of porphyrin 3

Porphyrin **2** (161.0 mg, 0.217 mmol) and KOH (36.6 mg, 0.652 mmol) were dissolved in a mixture of THF/ethanol 3:1 and heated to reflux for 3 h. Afterwards, the solvent was evaporated under reduced pressure. The crude product was dissolved in a mixture of THF/CH_2Cl_2 1:1 and washed with aqueous HCl (1 N) until pH 5 was reached. The product was extracted with water and the organic phase dried over $MgSO_4$ and concentrated under reduced pressure. The obtained solid was purified by recrystallization in methanol to afford porphyrin **3** as a purple solid (115.2 mg, 74%). ^1H NMR (δ ppm, 400 MHz, $CDCl_3$): 12.26 (s, br, 1H), 8.87–8.83 (m, 8H), 8.21 (m, 6H), 8.12 (d, J = 8.6 Hz, 2H), 7.80–7.72 (m, 9H), 4.28 (t, J = 6.2 Hz, 2H), 2.79 (t, J = 7.4 Hz, 2H), 2.38–2.30 (m, 2H), −2.77 (s, 2H). ^{13}C NMR (δ ppm, 100 MHz, $CDCl_3$): 173.5 (CO), 158.8, 142.4, 135.6, 134.8, 134.7, 129.3, 127.8, 126.8, 120.2, 120.1, 112.9, 60.7 (CH_2), 31.1 (CH_2), 24.0 (CH_2). FAB^+: m/z calculated for $C_{48}H_{36}N_4O_3$ $[M]^+$: 716.28 found $[M]^+$: 716.51. Elemental Anal. Calcd (%) for $C_{48}H_{36}N_4O_3$: C, 80.43; H, 5.06; N, 7.82. Found: C, 80.36; H, 5.03; N, 7.77.

2.3. Synthesis of the dendritic porphyrins including pyrene fragments 4a, 4b and 4c

2.3.1. Synthesis of porphyrin 4a

Porphyrin **3** (300.0 mg, 0.420 mmol) and 1-pyrenebutanol (137.6 mg, 0.502 mmol) were dissolved in anhydrous DMF (5 mL) at 5 °C. Then, 1-ethyl-3-(3-dimethylaminopropyl)carbodiimide (EDC) (96.5 mg, 0.502 mmol), *N*,*N*-diisopropylethylamine (DIPEA) (0.09 mL, 0.502 mmol) and hydroxybenzotriazole (HOBt) (67.8 mg, 0.502 mmol) were added. The reaction mixture was allowed to react at room temperature with stirring for 36 h. The solvent was removed under reduced pressure and the crude product was extracted with CH_2Cl_2/water. The organic phase was dried over $MgSO_4$ and the solvent was removed under reduced pressure. The crude product was purified by column chromatography using CH_2Cl_2 as eluent to obtain the desired product **4a** as a purple solid (235.9 mg, 57%). ^1H NMR (δ ppm, 400 MHz, $CDCl_3$): 8.87–8.83 (m, 8H), 8.28 (d, J = 8.4 Hz, 1H), 8.23 (d, J = 8.7 Hz, 6H), 8.12–8.06 (m, 6H), 7.97–7.88 (m, 4H), 7.80–7.73 (m, 9H), 7.23 (d, J = 8.3 Hz, 2H), 4.28–4.23 (m, 4H), 3.42 (t, J = 6.1 Hz, 2H), 2.69 (t, J = 7.4 Hz, 2H), 2.30–2.27 (m, 2H), 2.03–1.89 (m, 4H), −2.76 (s, 2H). ^{13}C NMR (δ ppm, 100 MHz, $CDCl_3$): 173.7 (CO), 159.0, 142.4, 136.6, 135.9, 134.9, 134.7, 131.2, 131.1, 130.2, 129.0, 128.1, 128.0, 127.6, 127.4, 126.1, 125.5, 125.3, 125.2, 125.17, 125.15, 124.9, 123.4, 120.2, 120.1, 112.9, 67.4 (CH_2), 64.8 (CH_2), 33.4 (CH_2), 31.7 (CH_2), 29.0 (CH_2), 28.5

(CH_2), 25.3 (CH_2). FAB$^+$: *m/z* calculated for $C_{68}H_{52}N_4O_3$ $[M]^+$: 972.40 found $[M]^+$: 972.62. Elemental Anal. Calcd (%) for $C_{68}H_{52}N_4O_3$: C, 83.92; H, 5.39; N, 5.76. Found: C, 83.96; H, 5.42; N, 7.73.

2.3.2. Synthesis of porphyrin 4b

Porphyrin **3** (300.0 mg, 0.420 mmol) and 1-aminopyrene (108.9 mg, 0.502 mmol) were dissolved in anhydrous DMF (5 mL) at 5 °C. Then, EDC (96.5 mg, 0.502 mmol), DIPEA (0.09 mL, 0.502 mmol) and HOBt (67.8 mg, 0.502 mmol) were added. The resulting reaction mixture was allowed to react at room temperature with stirring for 24 h. Then, the solvent was evaporated under reduced pressure and the crude product extracted with CH_2Cl_2/water. The organic phase was then dried with $MgSO_4$ and the solvent removed under vacuum. The crude product was purified by column chromatography using different mixtures of CH_2Cl_2/methanol, gradually increasing the polarity until a ratio of CH_2Cl_2/methanol 95:5 was reached. The desired product **4b** was obtained as a purple solid (295.3 mg, 77%). ^{1}H NMR (δ ppm, 400 MHz, $CDCl_3$): 8.87–8.80 (m, 8H), 8.52 (d, $J = 8.4$ Hz, 1H), 8.23 (d, $J = 8.7$ Hz, 6H), 8.20–7.97 (m, 10H), 7.83–7.75 (m, 9H), 7.38 (d, $J = 8.3$ Hz, 2H), 4.50 (t, $J = 6.1$ Hz, 2H), 3.04 (t, $J = 6.1$ Hz, 2H), 2.60–2.57 (m, 2H), −2.75 (s, 2H). ^{13}C NMR (δ ppm, 100 MHz, $CDCl_3$): 175.9 (CO), 150.8, 150.6, 150.5, 143.2, 135.9, 134.8, 131.2, 131.1, 130.2, 129.0, 128.1, 128.0, 127.6, 127.4, 126.1, 125.5, 125.3, 125.2, 125.17, 125.15, 124.9, 123.5, 120.2, 120.1, 112.9, 67.3 (CH_2), 33.1 (CH_2), 25.2 (CH_2). FAB$^+$: *m/z* calculated for $C_{64}H_{45}N_5O_2$ $[M]^+$: 915.36 found $[M]^+$: 915.69. Elemental Anal. Calcd (%) for $C_{64}H_{45}N_5O_2$: C, 83.91; H, 4.95; N, 7.64. Found: C, 83.86; H, 5.92; N, 7.60.

2.3.3. Synthesis of porphyrin 4c

Porphyrin **3** (300.0 mg, 0.420 mmol) and 1-pyrenemethylamine hydrochloride (134.9 mg, 0.502 mmol) were dissolved in anhydrous DMF (5 mL) at 5 °C. EDC (96.5 mg, 0.502 mmol), DIPEA (0.09 mL, 0.502 mmol) and HOBt (67.8 mg, 0.502 mmol) were added. The resulting reaction mixture was allowed to react at room temperature with stirring for 24 h. The solvent was evaporated at reduced pressure and the crude product extracted with CH_2Cl_2/water. The organic phase was then dried over $MgSO_4$ and the solution concentrated under reduced pressure. The crude product was purified by column chromatography using a mixture of hexanes/ethyl acetate 8:2. The desired product **4c** was obtained as a purple solid (306.5 mg, 66%). ^{1}H NMR (δ ppm, 400 MHz, $CDCl_3$): 8.85–8.79 (m, 8H), 8.33 (d, $J = 8.4$ Hz, 1H), 8.23–7.88 (m, 16H), 7.77–7.75 (m, 9H), 7.10 (d, $J = 8.3$ Hz, 2H), 5.23 (d, $J = 5.4$ Hz, 2H), 4.28–4.25 (m, 2H), 2.61–2.57 (m, 2H,), 2.38–2.34 (m, 2H), −2.77 (s, 2H). ^{13}C NMR (δ ppm, 100 MHz, $CDCl_3$): 172.3 (CO), 158.9, 142.6, 135.9, 134.9, 131.7, 131.6, 131.5, 131.1, 129.4, 128.7, 128.0, 127.9, 127.7, 127.0, 125.5, 125.3, 125.2, 125.17, 125.15, 124.9, 123.4, 120.2, 120.1, 112.9, 67.5 (CH_2), 42.5 (CH_2), 33.6 (CH_2), 25.9 (CH_2). FAB+: *m/z* calculated for $C_{65}H_{47}N_5O_2$ $[M]^+$: 929.37 found $[M]^+$: 929.80. Elemental Anal. Calcd (%) for $C_{65}H_{47}N_5O_2$: C, 83.94; H, 5.09; N, 7.53. Found: C, 83.96; H, 5.11; N, 7.48.

2.4. Synthesis of the dendritic Zn(II) 5a, 5b, 5c and Mg(II) 6a, 6b, 6c metalloporphyrins including pyrene fragments

2.4.1. Synthesis of Zn(II) metalloporphyrin 5a

Porphyrin **4a** (50.0 mg, 0.05 mmol) and $Zn(CH_3COO)_2{\cdot}2H_2O$ (47.2 mg, 0.257 mmol) were dissolved in anhydrous DMF (2 mL) under inert atmosphere and the resulting solution was heated to 110 °C. The reaction was monitored by UV–Vis spectroscopy until completion after 12 h. The purification of the metallated porphyrin was carried out by precipitation, using a mixture of CH_2Cl_2/hexanes. The product **5a** was then separated by filtration (50.1 mg, 94%). ^{1}H NMR (δ ppm, 400 MHz, $CDCl_3$): 8.94–8.91 (m, 8H), 8.26–8.21 (m, 7H), 8.09–7.93 (m, 10H), 7.80–7.73 (m, 9H), 7.23 (d, $J = 8.3$ Hz, 2H), 4.28–4.24 (m, 4H), 3.41 (t, $J = 6.1$ Hz, 2H), 2.69 (t, $J = 7.4$ Hz, 2H), 2.31–2.25 (m, 2H), 2.04–1.85 (m, 4H). ^{13}C NMR (δ ppm, 100 MHz, $CDCl_3$): 173.6 (CO), 159.0, 142.4, 136.6, 135.9, 134.9, 134.7, 131.2, 131.1, 130.2, 129.0, 128.2, 128.0, 127.6, 127.4, 126.1, 125.5, 125.3, 125.2, 125.17, 125.15, 124.9, 123.4, 120.4, 120.1, 112.9, 67.5 (CH_2), 64.8 (CH_2), 33.4 (CH_2), 31.7 (CH_2), 29.0 (CH_2), 28.6 (CH_2), 25.3 (CH_2). MALDI-TOF: *m/z* calculated for $C_{68}H_{50}N_4O_3Zn$ $[M]^+$: 1034.32 found $[M]^+$: 1034.47. Elemental Anal. Calcd (%) for $C_{68}H_{50}N_4O_3Zn$: C, 78.79; H, 4.86; N, 5.41. Found: C, 78.76; H, 4.89; N, 5.38.

2.4.2. Synthesis of the Zn(II) metalloporphyrin 5b

Metalloporphyrin **5b** was synthesized following the procedure described for metalloporphyrin **5a**. Porphyrin **4b** (50.0 mg, 0.055 mmol), $Zn(CH_3COO)_2{\cdot}2H_2O$ (50.1 mg, 0.275 mmol) and anhydrous DMF (2 mL). Reaction time 8 h. Metalloporphyrin **5b** was obtained as a purple solid (50.0 mg, 95%). ^{1}H NMR (δ ppm, 400 MHz, $CDCl_3$): 8.96–8.90 (m, 8H), 8.72–8.23 (m, 8H), 8.14–7.89 (m, 9H), 7.83–7.73 (m, 9H), 7.20 (d, $J = 8.3$ Hz, 2H), 4.33 (t, $J = 6.1$ Hz, 2H), 2.75 (t, $J = 6.1$ Hz, 2H), 2.36–2.34 (m, 2H). ^{13}C NMR (δ ppm, 100 MHz, $CDCl_3$): 175.8 (CO), 150.8, 150.5, 143.2, 135.9, 134.8, 131.2, 131.1, 130.2, 129.0, 128.1, 128.0, 127.6, 127.3, 126.1, 125.5, 125.3, 125.2, 125.18, 125,11, 124.9, 123.5, 120.2, 120.1, 112.9, 67.3 (CH_2), 33.2 (CH_2), 25.2 (CH_2). MALDI-TOF: *m/z* calculated for $C_{64}H_{43}N_5O_2Zn$ $[M]^+$: 977.27 found $[M]^+$: 977.44. Elemental Anal. Calcd (%) for $C_{64}H_{43}N_5O_2Zn$: C, 78.48; H, 4.43; N, 7.15. Found: C, 78.45; H, 4.39; N, 7.13.

2.4.3. Synthesis of the Zn(II) metalloporphyrin 5c

Metalloporphyrin **5c** was synthesized following the procedure described for metalloporphyrin **5a**. Porphyrin **4c** (15.0 mg, 0.016 mmol), $Zn(CH_3COO)_2{\cdot}2H_2O$ (16.1 mg, 0.080 mmol) and anhydrous DMF (2 mL). Reaction time 12 h. Metalloporphyrin **5c** was obtained as a purple solid (50.0 mg, 96%). ^{1}H NMR (δ ppm, 400 MHz, $CDCl_3$): 8.91–8.86 (m, 8H), 8.20–8.16 (m, 8H), 8.14–7.87 (m, 9H), 7.77–7.71 (m, 9H), 7.06 (d, $J = 8.3$ Hz, 2H), 5.34 (d, $J = 5.4$ Hz, 2H), 4.34 (t, $J = 6.1$ Hz, 2H), 2.47 (t, $J = 6.1$ Hz, 2H), 2.28–2.21 (m, 2H). ^{13}C NMR (δ ppm, 100 MHz, $CDCl_3$): 175.3 (CO), 150.9, 150.6, 150.5, 135.9, 134.96, 134.92, 131.7, 131.6, 131.5, 131.1, 129.4, 128.7, 128.0, 127.9, 127.7, 127.0, 125.5, 125.3, 125.2, 125.17, 125.15, 123.9, 123.4, 120.2, 120.1, 111.9, 67.6 (CH_2), 42.5 (CH_2), 33.6 (CH_2), 25.8 (CH_2). MALDI-TOF: *m/z* calculated for $C_{65}H_{45}N_5O_2Zn$ $[M]^+$: 991.29 found $[M]^+$: 991.46. Elemental Anal. Calcd (%) for $C_{65}H_{45}N_5O_2Zn$: C, 78.58; H, 4.57; N, 7.05. Found: C, 78.56; H, 4.53; N, 7.08.

2.4.4. Synthesis of the Mg(II) metalloporphyrin 6a

Porphyrin **4a** (50.0 mg, 0.051 mmol), $Mg(CH_3COO)_2{\cdot}4H_2O$ (570.7 mg, 2.550 mmol) and triethylamine (0.24 mL, 1.785 mmol) were dissolved in anhydrous DMF (3 mL) under inert atmosphere. The mixture was heated to 140 °C and the reaction progress monitored by UV–Vis spectroscopy until completion after 48 h. The solvent was evaporated and the crude metallated porphyrin was purified by precipitation using a mixture of CH_2Cl_2/hexanes. The product was separated by filtration. The metalloporphyrin **6a** was obtained as a green solid (49.5 mg, 96%). ^{1}H NMR (δ ppm, 400 MHz, $CDCl_3$): 9.00–8.97 (m, 8H), 8.32–8.28 (m, 7H), 8.15–7.89 (m, 10H), 7.86–7.78 (m, 9H), 7.28 (d, $J = 8.3$ Hz, 2H), 4.34–4.30 (m, 4H), 3.47 (t, $J = 6.1$ Hz, 2H), 2.75 (t, $J = 7.4$ Hz, 2H), 2.36–2.32 (m, 2H), 2.09–2.05 (m, 2H), 1.98–1.93 (m, 2H). ^{13}C NMR (δ ppm, 100 MHz, $CDCl_3$): 174.6 (CO), 150.8, 150.4, 137.6, 136.9, 134.9, 134.7, 131.2, 131.1, 130.2, 129.5, 128.4, 128.0, 127.6, 127.4, 126.1, 125.5, 125.3, 125.2, 125.17, 125.15, 124.9, 123.4, 120.4, 120.1, 112.9, 67.5 (CH_2), 64.8 (CH_2), 33.7 (CH_2), 31.7 (CH_2), 29.0 (CH_2), 28.6 (CH_2), 25.3 (CH_2). MALDI-TOF: *m/z* calculated for $C_{68}H_{50}N_4O_3Mg$ $[M]^+$: 994.37, found $[M]^+$: 994.56. Elemental Anal. Calcd (%) for $C_{68}H_{50}N_4O_3Mg$: C, 82.05; H, 5.06; N, 5.63. Found: C, 81.98; H, 5.04; N, 5.59.

2.4.5. Synthesis of the Mg(II) metalloporphyrin 6b

Metalloporphyrin **6b** was synthesized following the procedure described for metalloporphyrin **6a**. Porphyrin **4b** (50.0 mg, 0.055

mmol), $Mg(CH_3COO)_2{\cdot}4H_2O$ (584.2 mg, 2.730 mmol), triethylamine (0.27 mL, 1.910 mmol) and anhydrous DMF (3 mL). Reaction time 50 h. The metalloporphyrin **6b** was obtained as a green solid (49.5 mg, 95%). ^{1}H NMR (δ ppm, 400 MHz, $CDCl_3$): 8.96–8.94 (m, 8H), 8.23–8.20 (m, 7H), 8.13–7.79 (m, 10H), 7.78–7.72 (m, 9H), 7.29 (d, J = 8.3 Hz, 2H), 4.33 (t, J = 6.1 Hz, 2H), 2.75 (t, J = 6.1 Hz, 2H), 2.36–2.34 (m, 2H). ^{13}C NMR (δ ppm, 100 MHz, $CDCl_3$): 176.3 (CO), 151.4, 151.3, 150.5, 141.2, 136.9, 134.7, 131.1, 131.0, 130.2, 129.0, 128.1, 128.0, 127.6, 127.3, 126.1, 125.5, 125.3, 125.2, 125.18, 125.11, 124.9, 123.5, 120.2, 120.1, 112.9, 68.3 (CH_2), 34.2 (CH_2), 26.2 (CH_2). MALDI-TOF: *m/z* calculated for $C_{64}H_{43}N_5O_2Mg$ $[M]^+$: 937.33, found $[M]^+$: 937.53. Elemental Anal. Calcd (%) for $C_{64}H_{43}N_5O_2Mg$: C, 81.92; H, 4.62; N, 7.46. Found: C, 81.88; H, 4.58; N, 7.48.

2.4.6. Synthesis of the Mg(II) metalloporphyrin 6c

Metalloporphyrin **6c** was synthesized following the procedure described for metalloporphyrin **6a**. Porphyrin **4c** (15.0 mg, 0.016 mmol), $Mg(CH_3COO)_2{\cdot}4H_2O$ (172.6 mg, 0.800 mmol), triethylamine (0.80 mL, 0.560 mmol) and anhydrous DMF (3 mL). Reaction time 50 h. Metalloporphyrin **6c** was obtained as a green solid (14.8 mg, 96%). ^{1}H NMR (δ ppm, 400 MHz, $CDCl_3$): 8.85–8.78 (m, 8H), 8.33 (d, J = 8.4 Hz, 1H), 8.24–8.05 (m, 10H), 7.97–7.88 (m, 6H), 7.79–7.73 (m, 9H), 7.10 (d, J = 8.3 Hz, 2H), 5.21 (d, J = 6.8 Hz, 2H), 4.24 (t, J = 6.1 Hz, 2H), 2.57 (t, J = 6.1 Hz, 2H), 2.36–2.32 (m, 2H). ^{13}C NMR (δ ppm, 100 MHz, $CDCl_3$): 176.4 (CO), 151.3, 150.6, 150.3, 136.5, 134.9, 134.9, 131.8, 131.2, 131.1, 131.0, 129.4, 128.7, 128.0, 127.9, 127.8, 127.3, 127.0, 126.5, 125.3, 125.2, 125.1, 124.9, 123.9, 123.45, 121.4, 121.2, 111.9, 67.2 (CH_2), 42.4 (CH_2), 33.5 (CH_2), 25.7 (CH_2). FAB+: *m/z* calculated for $C_{65}H_{45}N_5O_2Mg$ $[M]^+$: 951.34, found $[M]^+$: 951.59. Elemental Anal. Calcd (%) for $C_{65}H_{45}N_5O_2Mg$: C, 81.97; H, 4.76; N, 7.35. Found: C, 81.95; H, 4.78; N, 7.33.

2.5. Synthesis of the dendritic porphyrins 7, 8 and 9

2.5.1. Synthesis of porphyrin 7

Porphyrin **3** (50.0 mg, 0.069 mmol) and di-*tert*-butyl 4-amino-4-[2-(*tert*-butoxycarbonyl)ethyl]heptanedioate (aminotriester) (43.5 mg, 0.139 mmol) were dissolved in anhydrous DMF (5 mL) at 5 °C [61,62]. Then, EDC (26.8 mg, 0.139 mmol), DIPEA (0.04 mL, 0.209 mmol) and HOBt (18.9 mg, 0.139 mmol) were added. The resulting reaction mixture was allowed to react with stirring at room temperature for 36 h. The solvent was evaporated under reduced pressure and the crude product extracted with a solvent mixture of CH_2Cl_2/water. The organic phase was dried over $MgSO_4$ and the solution concentrated under vacuum. The crude product was purified by column chromatography in silica gel, using hexanes/ethyl acetate 7:3 as eluent. The desired product **7** was obtained as a purple solid (63.5 mg, 82%). ^{1}H NMR (δ ppm, 400 MHz, $CDCl_3$): 8.92–8.79 (m, 8H), 8.22 (d, J = 8.4 Hz, 6H), 8.11 (d, J = 8.4 Hz, 2H), 7.81–7.72 (m, 9H), 7.29 (d, J = 8.4 Hz, 2H), 6.11 (s, 1H), 4.30 (t, J = 5.9 Hz, 2H), 2.51 (t, J = 7.3 Hz, 2H), 2.33–2.25 (m, 8H), 2.05 (dd, J = 8.9, 6.7 Hz, 6H), 1.45 (s, 27H), −2.77 (s, 2H). ^{13}C NMR (δ ppm, 100 MHz, $CDCl_3$): 173.4 (CO), 172.2 (CO), 159.1, 142.6, 136.0, 134.9, 134.7, 128.0, 127.1, 126.8, 120.2, 120.1, 112.9, 81.1 (C), 67.7 (C), 34.2 (CH_2), 31.3 (CH_2), 30.5 (CH_2), 30.3 (CH_2), 28.5 (CH_2), 25.9 (CH_3). FAB+: *m/z* calculated for $C_{70}H_{75}N_5O_8$ $[M]^+$: 1113.56, found $[M]^+$: 1113.85. Elemental Anal. Calcd (%) for $C_{70}H_{75}N_5O_8$: C, 75.45; H, 6.78; N, 6.28. Found: C, 75.41; H, 6.74; N, 6.30.

2.5.2. Synthesis of porphyrin 8

Porphyrin **7** (60.0 mg, 0.053 mmol) was dissolved in formic acid (2 mL) (98% v/v) under stirring for 12 h. The remaining acid was evaporated under reduced pressure and the product washed with toluene. The pure product was obtained as a purple solid (47.9 mg, 96%). ^{1}H NMR (δ ppm, 400 MHz, $CDCl_3$): 8.85 (m, 8H), 8.22 (d, J = 7.2 Hz, 6H), 8.12 (d, J = 8.2 Hz, 2H), 7.88–7.79 (m, 9H), 7.36 (d, J = 8.2 Hz, 2H), 4.25 (t, J = 6.3 Hz, 2H), 2.42 (t, J = 7.3 Hz, 2H), 2.23–2.14 (m, 6H), 2.12–2.09 (m, 2H), 1.96–1.84 (m, 6H), 1.22 (s, 3H), −2.92 (s, 2H). ^{13}C NMR (δ ppm, 100 MHz, $CDCl_3$): 175.3 (CO), 172.4 (CO), 159.4, 142.1, 136.1, 135.0, 134.1, 130.3 129.7, 129.0, 127.8, 126.1, 120.9, 120.7, 120.6, 68.1 (C), 57.3 (C), 33.2 (CH_2), 31.5 (CH_2), 29.9 (CH_2), 29.0 (CH_2), 26.1 (CH_2). FAB+: *m/z* calculated for $C_{58}H_{51}N_5O_8$ $[M]^+$: 947.39, found $[M]^+$: 947.90. Elemental Anal. Calcd (%) for $C_{58}H_{51}N_5O_8$: C, 73.63; H, 5.43; N, 7.40. Found: C, 73.60; H, 5.40; N, 7.36.

2.5.3. Synthesis of porphyrin 9

Porphyrin **8** (50.0 mg, 0.058 mmol), 1-pyrenemethylamine chlorhydrate ($PyCH_2NH_2$) (46.6 mg, 0.174 mmol), (2-(1*H*-benzotriazol-1-yl)-1,1,3,3-tetramethyluronium hexafluorophosphate (HBTU) (88.0 mg, 0.232 mmol) and DIPEA (0.12 mL, 0.696 mmol) were dissolved in anhydrous DMF (3 mL) under inert atmosphere. The resulting mixture was stirred at room temperature for 36 h, concentrated under reduced pressure and redissolved in CH_2Cl_2. The organic phase was washed with water and the resulting solution dried over $MgSO_4$ and concentrated under reduced pressure. The crude product was purified by column chromatography in silica gel, using a solvent mixture of CH_2Cl_2/methanol 95:5 as eluent. The desired product **9** was obtained as a purple solid (45.8 mg, 50%). ^{1}H NMR (δ ppm, 400 MHz, $CDCl_3$): 8.88–8.85 (m, 4H), 8.76 (d, J = 4.8 Hz, 2H), 8.69 (d, J = 4.8 Hz, 2H), 8.22–8.19 (m, 6H), 7.88–7.62 (m, 38H), 6.95 (d, J = 8.2 Hz, 2H), 6.87 (s, 1H), 6.49 (t, J = 5.4 Hz, 3H), 4.77 (d, J = 5.4 Hz, 6H), 3.86 (t, J = 5.9 Hz, 2H), 2.31 (t, J = 7.2 Hz, 2H), 2.25 (t, J = 7.5 Hz, 6H), 2.14–2.05 (m, 6H), 2.00–1.96 (m, 2H), −2.84 (s, 2H). ^{13}C NMR (δ ppm, 100 MHz, $CDCl_3$): 190.6 (CO), 173.1 (CO), 142.0, 136.2, 136.1, 136.0, 135.2, 131.5, 131.1, 130.3, 130.1, 129.7, 129.0, 128.8, 127.8, 127.7, 127.6, 127.4, 126.9, 126.1, 125.3, 125.2, 125.1, 125.0, 124.9, 123.4, 120.9, 120.7, 120.6, 79.9 (C), 57.9 (C), 41.2 (CH_2), 33.2 (CH_2), 31.5 (CH_2), 31.3 (CH_2), 29.9 (CH_2), 26.1 (CH_2). MALDI-TOF: *m/z* calculated for $C_{109}H_{84}N_8O_5$ $[M]^+$: 1585.88 found $[M]^+$: 1586.25. Anal. Calcd (%) for $C_{109}H_{84}N_8O_5$: C, 82.55; H, 5.34; N, 7.07. Found: C, 82.51; H, 5.36; N, 7.03.

2.6. Metallation of the dendritic porphyrin 9

2.6.1. Synthesis of the Zn(II) metalloporphyrin 10

Metalloporphyrin **10** was synthesized following the procedure described for metalloporphyrin **5a.** Porphyrin **9** (16.0 mg, 0.010 mmol), $Zn(CH_3COO)_2{\cdot}2H_2O$ (18.5 mg, 0.102 mmol) and anhydrous DMF (2 mL). Reaction time 12 h. The metallated porphyrin **10** was obtained as a purple solid (45.8 mg, 50%). ^{1}H NMR (δ ppm, 400 MHz, $CDCl_3$): 8.88–8.85 (m, 4H), 8.76 (d, J = 4.8 Hz, 2H), 8.69 (d, J = 4.8 Hz, 2H), 8.22–8.19 (m, 6H), 7.88–7.62 (m, 38H), 6.95 (d, J = 8.2 Hz, 2H), 6.87 (s, 1H), 6.49 (t, J = 5.4 Hz, 3H), 4.77 (d, J = 5.4 Hz, 6H), 3.86 (t, J = 5.9 Hz, 2H), 2.31 (t, J = 7.2 Hz, 2H), 2.25 (t, J = 7.5 Hz, 6H), 2.14–2.05 (m, 6H), 2.00–1.96 (m, 2H), −2.84 (s, 2H). 8.82–8.71 (m, 8H), 8.53 (t, J = 5.7 Hz, 3H), 8.21–7.73 (m, 44H), 7.43 (s, 1H), 7.29 (d, J = 8.2 Hz, 2H), 4.92 (d, J = 5.5 Hz, 6H), 4.19 (t, J = 6.5 Hz, 2H), 2.38 (t, J = 7.2 Hz, 2H), 2.24–2.20 (m, 6H), 2.11–1.98 (m, 8H). ^{13}C NMR (δ ppm, 100 MHz, $CDCl_3$): 189.3 (CO), 172.4 (CO), 142.1, 136.3, 136.2, 136.0, 135.2, 131.6, 131.2, 130.15, 130.11, 129.7, 129.5, 128.9, 127.9, 127.7, 127.6, 127.4, 126.9, 126.18, 126.13, 125.3, 125.2, 125.1, 125.0, 124.9, 123.4, 120.9, 120.7, 120.6, 81.1(C), 57.8 (C), 41.1 (CH_2), 33.3 (CH_2), 31.6 (CH_2), 31.3 (CH_2), 29.9 (CH_2), 25.7 (CH_2). MALDI-TOF: *m/z* calculated for $C_{109}H_{82}N_8O_5Zn$ $[M]^+$: 1649.25, found $[M]^+$: 1649.43. Calcd (%) for $C_{109}H_{82}N_8O_5Zn$: C, 79.38; H, 5.01; N, 6.79. Found: C, 79.41; H, 4.98; N, 6.77.

3. Results and discussion

3.1. Synthesis

The synthesis of the zero generation pyrene porphyrin derivatives **4a** to **4c** is shown in Scheme 1. 4-Hydroxybenzaldehyde was reacted in the presence of ethyl 4-bromobutyrate under Williamson reaction

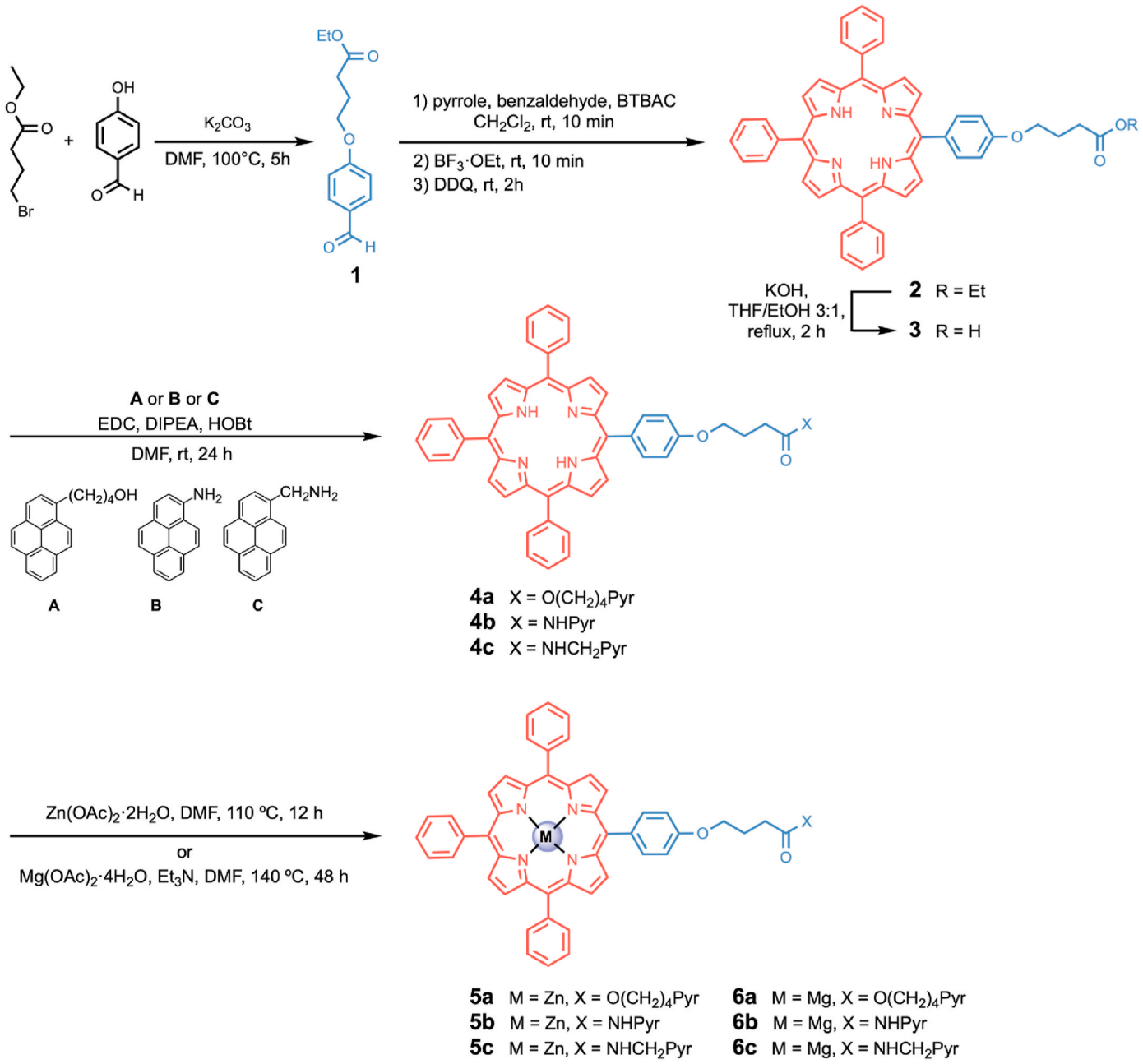

Scheme 1. Synthesis of zero generation pyrene dendronized porphyrins **4a**–**4c**, and metallated complexes **5a**–**5c** and **6a**–**6c**.

conditions to give intermediate ethyl-4-(4-formylphenoxy) butanoate (**1**) [60]. To construct the porphyrin core, the methodology reported by Lindsey and coworkers was followed [63–65]. Compound **1** was reacted in the presence of benzaldehyde and pyrrole using $BF_3{\cdot}OEt_2$ as catalyst at highly diluted concentration, followed by an oxidation with DDQ to obtain the desired porphyrin compound **2** [39]. Compound **2** was hydrolyzed under basic conditions to give the corresponding carboxylic acid **3**. For the synthesis of **4a**, **4b** and **4c**, compound **3** was esterified using EDC, HOBt and DIPEA in the presence of 1-pyrenebutanol, 1-aminopyrene and 1-pyrenemethylamine, respectively.

First generation of Newkome type pyrene dendronized porphyrin **9** (Scheme 2) was synthesized starting from the esterification of compound **3** with aminotriester to give porphyrin **7** [61,62]. Hydrolysis of compound **7** under basic conditions gave compound **8**. Pyrene was incorporated through amide formation using HBTU and DIPEA in the presence of 1-pyrenemethylamine to obtain first generation pyrene dendronized porphyrin **9**.

Metallation reactions were performed as previously reported by us [41]. Zinc acetate was used to metallate zero and first generation pyrene dendronized porphyrins, while magnesium acetate was used to metallate the zero generation porphyrins (Scheme 1 and Scheme 2). The complexation reactions were monitored by UV–Vis spectroscopy. The coordination was confirmed by the disappearance of two Q bands together with a red shift of the Soret band.

3.2. Characterization of the compounds

Analysis by ^{1}H NMR of all the pyrene dendronized porphyrins produced similar NMR spectra (Fig. 1). All compounds exhibited two signals between $\delta = 8.90$ and 8.70 ppm, corresponding to the protons of the porphyrin core, whereas signals due to the phenyl groups were observed at $\delta = 8.23$ and 7.76 ppm.

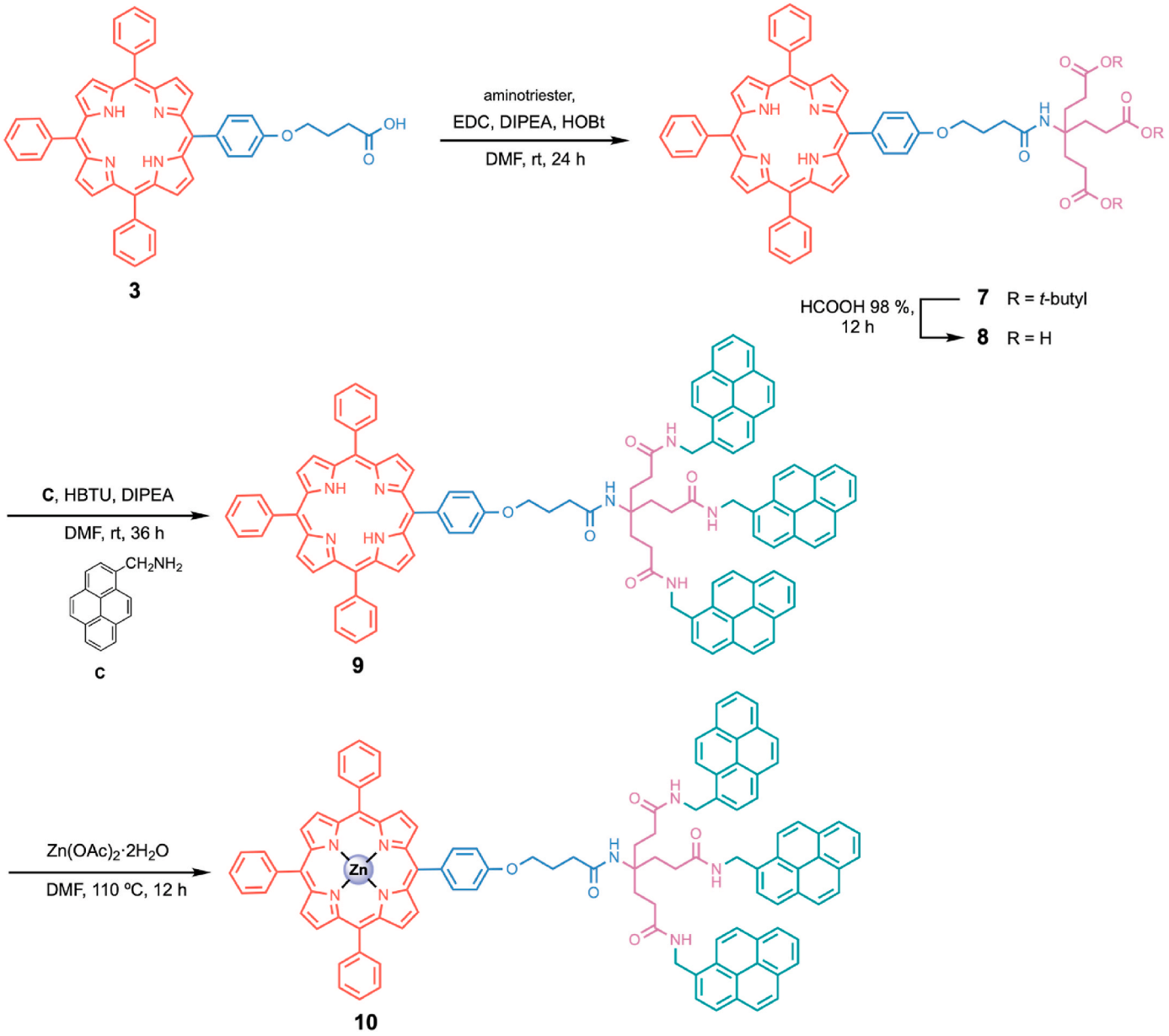

Scheme 2. Synthesis of first generation pyrene dendronized porphyrins **9** and **10**.

In addition, for the compounds including the pyrene units (compounds **4a–c** and **9**), signals of the protons of this moiety were observed between $\delta = 8.40$ and 7.70 ppm and partially overlapped with those of the porphyrin moiety. A signal corresponding to the protons at the *meso* position of the porphyrin substituted benzylic ring can be observed between $\delta = 7.10$ and 7.00 ppm. Furthermore, for all compounds three more signals were observed in the aliphatic region due to the ethyl 4-(4-formylphenoxy) butanoate fragment at $\delta = 4.30$, 2.60 and 2.30 ppm, with slight shift variations for the different compounds. Additionally, in the case of 1-pyrenebutanol, a series of aliphatic signals can be observed at $\delta = 3.40$, 2.00 and 1.90 ppm. When 1-pyrenemethylamine was employed as spacer, a signal due to the methylene group was observed at $\delta = 5.20$–4.80 ppm. The dendritic porphyrin compounds **7** to **10,** showed two signals corresponding to the methylene groups of the aliphatic chain between $\delta = 2.30$ and 2.05 ppm. Finally, a signal at −2.70 ppm (which shifts to −2.80 ppm in some of the compounds), corresponding to the inner protons of the free-base porphyrins was also observed. This signal completely disappeared once the porphyrins have been metallated, being a clear indication that the inner protons have been replaced by the metal. The characterization of the whole series of compounds was complemented by FAB^+, MALDI-TOF mass spectrometry and elemental analyses. All these results are in agreement with the proposed structures.

3.3. Optical properties of the studied compounds

The optical properties of the pyrene dendronized porphyrins were determined by absorption spectroscopy in the UV–vis range in THF solution. This solvent was selected since the obtained dendritic compounds are totally soluble, avoiding the formation of aggregates. Moreover, the use of viscous solvents such as DMSO or DMF was avoided since they slow down the encounter between the donor (pyrene) and the acceptor (porphyrin) groups thereby affecting the velocity and making more difficult the energy transfer (FRET).

The optical properties of the compounds are summarized in Table 1. All compounds exhibit the $S_0 \rightarrow S_2$ band of pyrene at 344 nm, as well as the typical bands of the porphyrin: a Soret band at about 418 nm, followed by four Q bands between 450 and 700 nm for the free-base

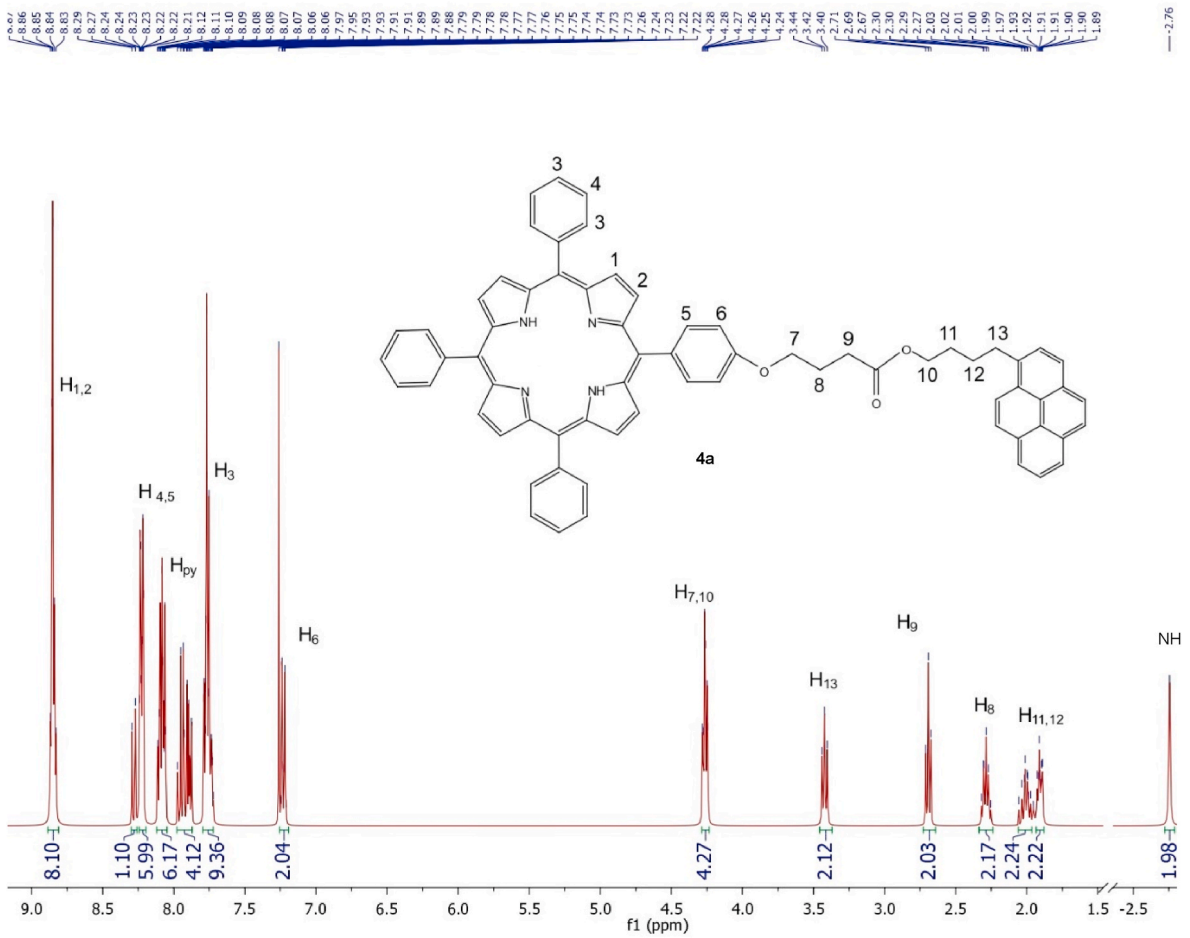

Fig. 1. ^{1}H NMR spectrum and assignment of signals for compound **4a**.

Table 1
Optical properties of the series of compounds.

Compound	Pyrene and Soret bands		Q bands
	λ (nm)[a]	ε (M^{-1} cm^{-1})[b]	λ (nm)[a]
2	418	486,000	513, 548, 593, 647
4a	344	50,000	514, 550, 592, 648
	418	459,500	
4b	344	44,000	515, 550, 592, 648
	418	452,000	
4c	344	54,000	514, 548, 592, 648
	418	443,000	
5a	344	42,000	557, 596
	424	565,000	
5b	345	35,000	556, 596
	424	452,000	
5c	344	46,000	556, 596
	424	457,000	
6a	344	51,500	571, 613
	430	504,000	
6b	344	36,5000	572, 612
	430	452,000	
6c	344	52,500	572, 614
	430	474,500	
9	344	141,500	514, 548, 592, 648
	418	493,500	
10	344	132,000	555, 597
	424	440,000	

[a] Maximum absorption wavelength for pyrene, Soret band and Q bands of each compound.
[b] Molar extinction coefficient calculated for pyrene and Soret band.

porphyrins and only two Q bands for the metalloporphyrins.

The obtained absorption spectra of the pyrene dendronized porphyrins bearing butylpyrenyl (**4a, 5a, 6a)** and methynepyrenyl (**4c, 5c, 6c** and **9**) groups correspond to the sum of the absorption bands of pyrene and porphyrin moieties, which suggests that there is no significant interaction between both chromophores in the ground state. Interestingly, dendronized porphyrins bearing pyrene directly linked to

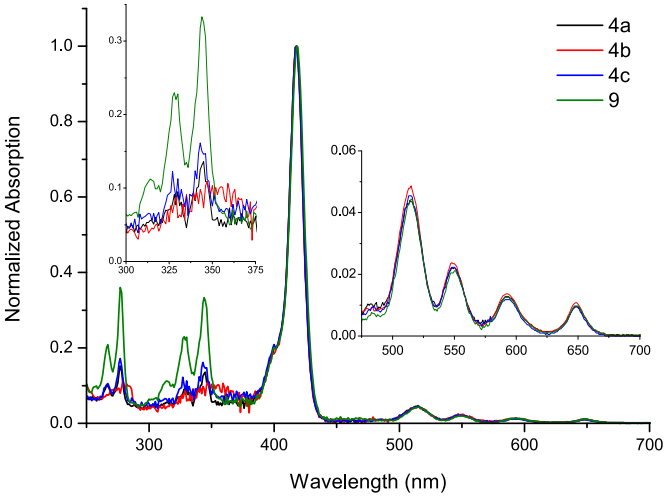

Fig. 2. Normalized absorption spectra of the free-base pyrene dendronized porphyrins (**4a**, **4b**, **4c**, and **9**) in THF.

amide group (**4b**, **5b** and **6b**), showed a significant broadening in the absorption band of the pyrene, caused by electron delocalization. In Fig. 2, the absorption spectra of zero and first generation pyrene dendronized porphyrins **4a–c** and **9**, respectively is presented.

The molar extinction coefficients (ε) were calculated using the Beer-Lambert law by plotting a curve of absorbance *vs* concentration and the results are shown in Table 1. The obtained values for the molar extinction coefficients of the Soret band of the porphyrin moiety are comprised between 443,500 and 486,000 M^{-1} cm^{-1}, which is in accordance with the reported ε value of the tetraphenylporphyrin (470,000 M^{-1} cm^{-1}) [66].

In the absorption spectra of all pyrene dendronized porphyrins, a bathochromic shift of the Soret band was observed after the metallation with either zinc or magnesium (Fig. 3). In all cases the band corresponding to the pyrene moiety was not affected, and the presence of only two Q bands confirmed that the coordination with the metal occurred.

Finally, compounds **9** and **10** behaved similarly exhibiting a higher molar extinction coefficient value for the absorption band at 344 nm than their generation zero analogs, since the number of pyrenes is significantly increased (Fig. 4). The absorbance ratio A_{py} (344 nm)/A_{por} (Soret 418 nm) for the zero and first generation pyrene dendronized porphyrins, **4c** and **9** was calculated to be 0.11 and 0.29, respectively. Being the A_{py}/A_{por} value for compound **9** three times higher due to its three-fold pyrene content.

3.4. Emission properties of the studied compounds

The fluorescence emission spectra were recorded in THF (A = 0.05) at room temperature. The excitation wavelengths were 344 nm for the $S_0 \rightarrow S_2$ transition of the pyrene moiety, 418, 424, and 430 nm for the Soret band of the free-base, Zn(II)- and Mg(II)-metallated porphyrins, respectively. The obtained emission spectra are shown in Fig. 5.

The free-base porphyrin **4c** exhibited a $S_{(1,0)} \rightarrow S_{(0,0)}$ emission band at 653 nm (Fig. 5A). This band was blue shifted to 603 nm in the Zn(II) metallated compound **5c** and to 618 nm for the Mg(II) derivative **6c**. The second emission band of lower energy appeared at 715 nm for the free-base porphyrin **4c**, whereas this band was blue-shifted for the Zn(II) and Mg(II) metallated porphyrins, **5c** and **6c**, exhibiting this band at 654 and 673 nm, respectively.

When these compounds were excited at 344 nm (Fig. 5B), residual pyrene monomer emission was observed at 375 nm, followed by the emission of the porphyrin moiety. This last emission revealed that an energy transfer phenomenon is occurring from pyrene to porphyrin.

The quantum yields of the pyrene dendronized porphyrins were determined using the following equation [67]:

$$\Phi_{F_{(x)}} = \left(\frac{A_s}{A_x}\right)\left(\frac{F_x}{F_s}\right)\left(\frac{n_x}{n_x}\right)^2 \Phi_{F_{(s)}} \quad (1)$$

where s stands for standard and x for sample, A is the absorbance at the excitation wavelength, F is the area under the emission spectra, n is the refraction index of the solvent and $\Phi_{F(s)}$ is the quantum yield of the standard. To determine the quantum yield, a quinine solution in H_2SO_4 (1 M) was employed ($\Phi = 0.55$) as a standard for the pyrene moiety and tetraphenylporphyrin in toluene ($\Phi = 0.11$) was used for the porphyrin core [68,69]. The results are summarized in Table 2.

3.5. FRET efficiency of the compounds

The FRET efficiency (E_{FRET}) was calculated for all compounds and resulted to be almost quantitative. The results showed that there is an efficient energy transfer phenomenon from the donor (pyrene) to the acceptor (porphyrin), when the donor is excited at 344 nm. From the analysis of the emission spectra, it was observed that the pyrene emission (λ_{ex} = 344 nm) decreases considerably from a quantum yield value of 0.542 for 1-pyrenebutanol to about 0.003, with the appearance of the emission bands of the porphyrin. The calculated FRET efficiencies were

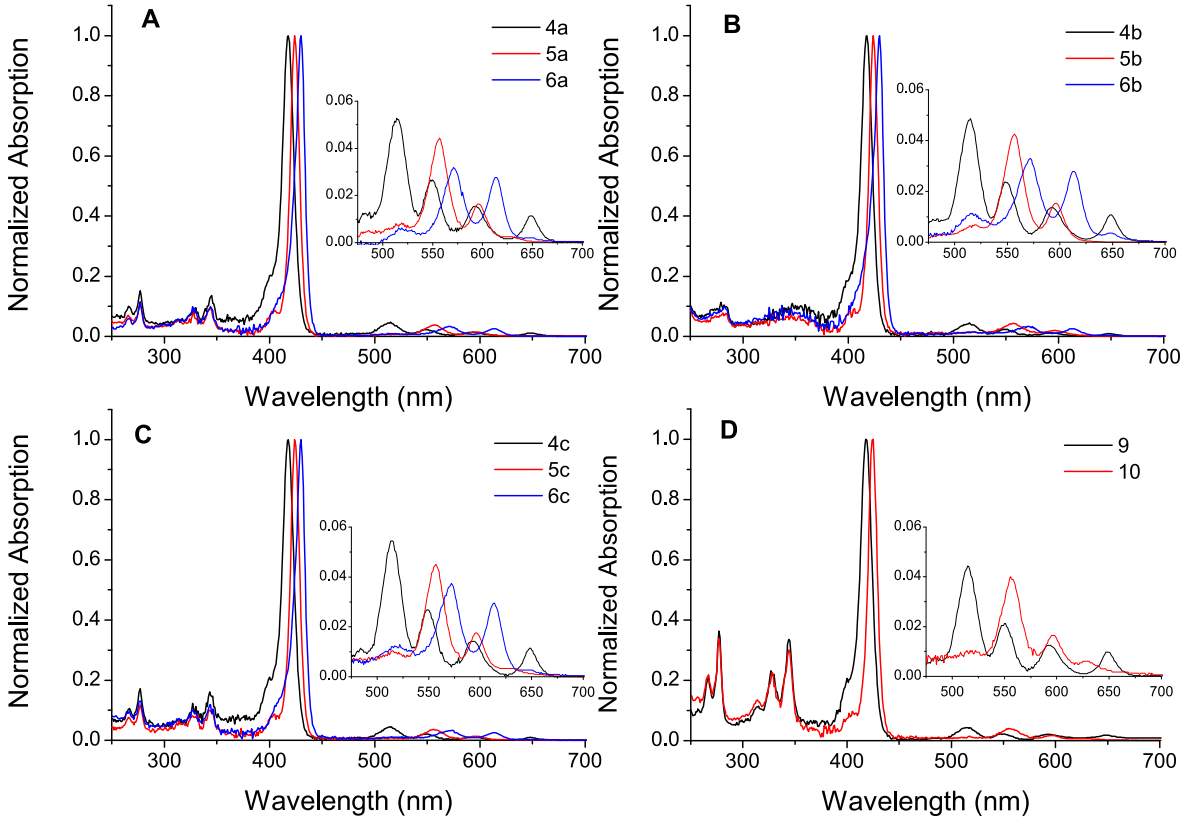

Fig. 3. Normalized absorption spectra recorded in THF.

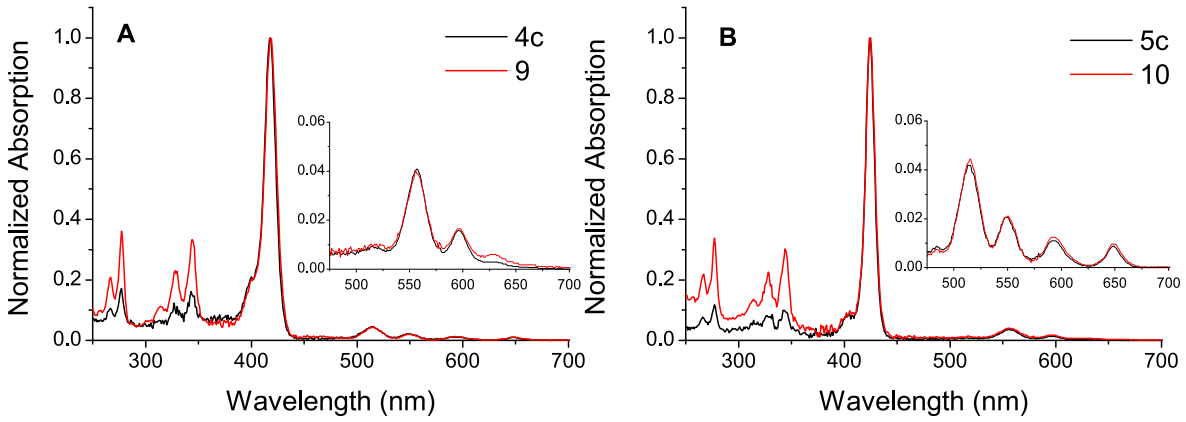

Fig. 4. Comparison of normalized absorption spectra of zero and first generation pyrene dendrimers recorded in THF.

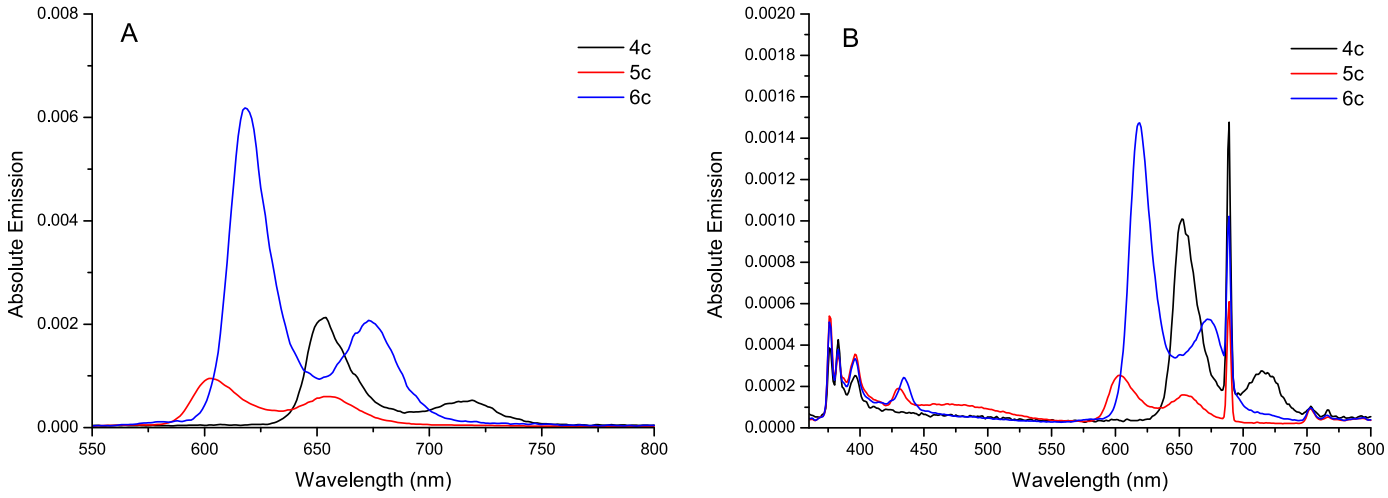

Fig. 5. Absolute emission spectra recorded in THF for the free-base **4c** and metallated porphyrins **5c** and **6c**. **A)** Excitation wavelength corresponding to the Soret band (see Table 1). **B)** Excitation wavelength 344 nm. The sharp peak at 688 nm corresponds to the harmonic (double the excitation wavelength).

Table 2
Quantum yields and FRET efficiency of the compounds.

Compound	$\lambda_{emission\text{-}max}$ (nm)[a]		Φ (pyrene) λ_{ex} = 344 nm	Φ (porphyrin) λ_{ex} = 344 nm	Φ (porphyrin) λ_{ex} = Soret band[b]	E_{FRET} (%)[c]
PyOH[d]	375	–	0.542	–	–	–
4a	375	651	0.002	0.047	0.091	99.6
4b	376	652	0.002	0.053	0.093	99.6
4c	375	652	0.002	0.065	0.086	99.5
5a	375	602	0.003	0.037	0.075	99.5
5b	376	603	0.003	0.035	0.058	99.5
5c	375	603	0.003	0.032	0.063	99.5
6a	375	618	0.003	0.102	0.159	99.5
6b	376	618	0.003	0.086	0.251	99.5
6c	375	618	0.003	0.086	0.243	99.5
9	376	652	0.003	0.032	0.089	99.4

[a] Emission wavelengths for the pyrene and the Soret bands of each compound.
[b] Excitation at absorption wavelength corresponding to the Soret band (See Table 1).
[c] FRET efficiencies were calculated using the following equation: FRET = 1 – (I_{DA}/I_D), where I_{DA} is the integration of the residual emission of the donor when linked to the acceptor and I_D is the integration of the emission of the donor in the absence of the acceptor.
[d] 1-Pyrenebutanol.

above 99%. The flexibility of the structures of the pyrene dendronized porphyrins of zero and first generations allowed the encounter of donor and acceptor chromophores favoring the energy transfer. Moreover, as previously reported by our group, no excimer emission was observed from the pyrene moiety [41,43]. This is due to the rate constant of the energy transfer is much faster than the rate constant for the excimer formation.

The optical properties of these flexible free-base and metallated dendronized porphyrins were compared to those of a previously reported series bearing more rigid structures. When comparing zero generation dendronized porphyrins (free base **4a-c**, Zn-metallated **5a-c** and Mg-metallated **6a-c**) to their rigid homologues (Ref [41]: free base **3**, Zn-metallated **3a** and Mg-metallated **3c**), it can be observed that the absorption and emission wavelengths are very similar. In the case of the first generation dendronized porphyrins, the flexible dendritic molecule reported here (free-base **9**) and its homologue with a more rigid dendronized porphyrin (Ref [41]: free-base **4**) presented similar absorption and emission wavelengths. However, the flexible dendronized porphyrins reported in this work exhibited higher E_{FRET}, with values between 99.4 -99.6%, than the more rigid dendronized porphyrins previously reported [41], which showed E_{FRET} values between 96 and 99%. From these results, it was concluded that better E_{FRET} were reached with more flexible structures, which facilitate the encounter between the donor and acceptor groups in the dendritic molecules.

4. Conclusions

A novel series of zero and first generation dendritic compounds, bearing peripheral pyrene groups and a porphyrin core connected with spacers of different lengths, were synthesized and fully characterized. These compounds were further metallated with Zn(II) and Mg(II), as was evidenced by UV–vis absorption where two porphyrin Q bands were observed instead of the four bands observed for the free-base porphyrin. The Soret absorption band of the metallated compounds exhibited a red shift compared with their free-base analogs, whereas, the emission band was blue shifted. When excited at 344 nm, emission of the porphyrin moiety and low intensity residual emission of pyrene were observed. This was a clear indication that FRET occurred. All the studied compounds showed outstanding energy transfer efficiencies, reaching E_{FRET} values above 99%.

Author statement

Yoliztli Bañales-Leal: Investigation, Data Curation, Validation, Formal Analysis, Visualization **Andrea García-Rodríguez**: Methodology, Investigation, Formal Analysis **Fabián Cuétara-Guadarrama**: Methodology, Visualization, Writing - Review & Editing **Mireille Vonlanthen**: Methodology, Visualization, Investigation, Writing - Review & Editing **Kendra Sorroza-Martínez**: Investigation, Data Curation, Formal Analysis. **David Morales-Morales:** Resources, Writing Original Draft, Supervision, Project Administration **Ernesto Rivera**: Resources, Writing Original Draft, Supervision, Project Administration, Funding Acquisition.

Declaration of competing interest

The authors declare that they have no known competing financial interests or personal relationships that could have appeared to influence the work reported in this paper.

Acknowledgements

The authors are grateful to Miguel Ángel Canseco, Gerardo Cedillo, María de los Ángeles Peña González and Elizabeth Huerta Salazar for the technical assistance in the characterization of the compounds. Lucero Ríos and Carmen García for MALDI-TOF measurements. We are grateful to PAPIIT-DGAPA (Project IN101119) and CONACyT (Project 279380) for the financial support.

References

[1] Tomalia DA, Naylor AM, Goddard WA. Starburst dendrimers: molecular-level control of size, shape, surface chemistry, topology, and flexibility from atoms to macroscopic matter. Angew Chem Int Ed Engl 1990;29(2):138–75.
[2] Bosman AW, Janssen HM, Meijer EW. About dendrimers: structure, physical properties, and applications. Chem Rev 1999;99(7):1665–88.
[3] Fischer M, Vogtle F. Dendrimers: from design to application - a progress report. Angew Chem Int Ed Engl 1999;38(7):884–905.
[4] Astruc D. Electron-transfer processes in dendrimers and their implication in biology, catalysis, sensing and nanotechnology. Nat Chem 2012;4(4):255–67.
[5] Caminade AM, Turrin CO, Laurent R, Ouali A, Delavaux-Nicot B. Dendrimers: towards catalytic, material and biomedical uses. Chichester: John Wiley & Sons. Inc; 2011.
[6] Astruc D, Boisselier E, Ornelas C. Dendrimers designed for functions: from physical, photophysical, and supramolecular properties to applications in sensing, catalysis, molecular electronics, photonics, and nanomedicine. Chem Rev 2010;110(4):1857–959.
[7] Sun HJ, Zhang S, Percec V. From structure to function via complex supramolecular dendrimer systems. Chem Soc Rev 2015;44(12):3900–23.
[8] Mignani S, Rodrigues J, Tomas H, Zablocka M, Shi X, Caminade AM, Majoral JP. Dendrimers in combination with natural products and analogues as anti-cancer agents. Chem Soc Rev 2018;47(2):514–32.
[9] Caminade AM, Laurent R. Homogeneous catalysis with phosphorus dendrimer complexes. Coord Chem Rev 2019;389:59–72.
[10] Pedziwiatr-Werbicka E, Milowska K, Dzmitruk V, Ionov M, Shcharbin D, Bryszewska M. Dendrimers and hyperbranched structures for biomedical applications. Eur Polym J 2019;119:61–73.
[11] Tomalia DA, Nixon LS, Hedstrand DM. The role of branch cell symmetry and other critical nanoscale design parameters in the determination of dendrimer encapsulation properties. Biomolecules 2020;10(4):642.
[12] Ceroni P, Bergamini G, Marchioni F, Balzani V. Luminescence as a tool to investigate dendrimer properties. Prog Polym Sci 2005;30(3–4):453–73.
[13] Nantalaksakul A, Reddy DR, Bardeen CJ, Thayumanavan S. Light harvesting dendrimers. Photosynth Res 2006;87(1):133–50.
[14] Adronov A, Fréchet JMJ. Light-harvesting dendrimers. Chem Commun 2000;1701–10.
[15] Balzani V, Ceroni P, Maestri M, Vicinelli V. Light-harvesting dendrimers. Curr Opin Chem Biol 2003;7(6):657–65.
[16] Abd-El-Aziz AS, Abdelghani AA, Wagner BD, Bissessur R. Advances in light-emitting dendrimers. Macromol Rapid Commun 2019;40(1):1800711.
[17] Winnik F. Photophysics of preassociated pyrenes in aqueous polymer solutions and in other organized media. Chem Rev 1993;93(2):587–614.
[18] Figueira-Duarte TM, Müllen K. Pyrene-based materials for organic electronics. Chem Rev 2011;111(11):7260–314.
[19] Duhamel J. Internal dynamics of dendritic molecules probed by pyrene excimer formation. Polymers 2012;4(1):211–39.
[20] Duhamel J. Polymer chain dynamics in solution probed with a fluorescence blob model. Acc Chem Res 2006;39(12):953–60.
[21] Duhamel J. New insights in the study of pyrene excimer fluorescence to characterize macromolecules and their supramolecular assemblies in solution. Langmuir 2012;28(16):6527–38.
[22] Yip J, Duhamel J, Bahun GJ, Adronov A. A study of the dynamics of the branch ends of a series of pyrene-labeled dendrimers based on pyrene excimer formation. J Phys Chem B 2010;114(32):10254–65.
[23] Raimbault J, Casier R, Little H, Duhamel J. Hydrophobic and elastic forces experienced by a series of pyrene end-labeled poly(ethylene oxide)s interacting with sodium dodecyl sulfate micelles. Macromolecules 2018;51(15):5933–43.
[24] Cicchi S, Fabbrizzi P, Ghini G, Brandi A, Foggi P, Marcelli A, Righini R, Botta C. Pyrene-excimers-based antenna systems. Chem Eur J 2009;15(3):754–64.
[25] Rivera E, Aguilar-Martínez M, Terán G, Flores RF, Bautista-Martínez JA. Thermal, optical, electrochemical properties and conductivity of trans- and cis-poly(1-ethynylpyrene): a comparative investigation. Polymer 2005;46(13):4789–98.
[26] Illescas J, Caicedo C, Zaragoza-Galán G, Ramírez-Fuentes YS, Gelover-Santiago A, Rivera E. Synthesis, characterization and optical properties of novel well-defined di(1-ethynylpyrene)s. Synth Met 2011;161(9–10):775–82.
[27] Hall T, Whitton G, Casier R, Gauthier M, Duhamel J. Arborescent poly(l -glutamic acid)s as standards to study the dense interior of polypeptide mesoglobules by pyrene excimer fluorescence. Macromolecules 2018;51(20):7914–23.
[28] Anderson HL. Building molecular wires from the colours of life: conjugated porphyrin oligomers. Chem Commun 1999:2323–30.
[29] DeRosa MC, Crutchley RJ. Photosensitized singlet oxygen and its applications. Coord Chem Rev 2002;233–234:351–71.
[30] Bozja J, Sherrill J, Michielsen S, Stojiljkovic I. Porphyrin-based, light-activated antimicrobial materials. J Polym Sci Part A Polym Chem 2003;41(15):2297–303.
[31] Krieger A, Fuenzalida Werner JP, Mariani G, Gröhn F. Functional supramolecular porphyrin-dendrimer assemblies for light harvesting and photocatalysis. Macromolecules 2017;50(9):3464–75.
[32] Chen J, Fan T, Xie Z, Zeng Q, Xue P, Zheng T, Xue P, Zheng T, Chen Y, Luo X, Zhang H. Advances in nanomaterials for photodynamic therapy applications: status and challenges. Biomaterials 2020;237:119827.
[33] Aratani N, Kim D, Osuka A. Discrete cyclic porphyrin arrays as artificial light-harvesting antenna. Acc Chem Res 2009;42(12):1922–34.
[34] Choi MS, Aida T, Yamazaki T, Yamazaki I. Dendritic multiporphyrin arrays as light-harvesting antennae: effects of generation number and morphology on intramolecular energy transfer. Chem Eur J 2002;8(12):2667–78.
[35] Yim D, Sung J, Kim S, Oh J, Yoon H, Sung YM, Kim D, Jang WD. Guest-induced modulation of the energy transfer process in porphyrin-based artificial light harvesting dendrimers. J Am Chem Soc 2017;139(2):993–1002.
[36] Li WS, Aida T. Dendrimer porphyrins and phthalocyanines. Chem Rev 2009;109(11):6047–76.
[37] Dandliker PJ, Diederich F, Zingg A, Gisselbrecht JP, Gross M, Louati A, Sanford E. Dendrimers with porphyrin cores: synthetic models for globular heme proteins. 121 Helv Chim Acta 1997;80(6):1773–801.
[38] Rodríguez-Alba E, Ortíz-Palacios J, Vonlanthen M, Rojas-Montoya SM, Porcu P, Ruiu A, Rivera E. Design of novel well-defined oligothiophenes bearing donor-acceptor groups (pyrene-porphyrin): synthesis, characterization, optical properties and energy transfer. J Mol Struct 2019;1183:28–36.
[39] Vonlanthen M, Gonzalez-Ortega J, Porcu P, Ruiu A, Rodríguez-Alba E, Cevallos-Vallejo A, Rivera E. Pyrene-labeled dendrimers functionalized with fullerene C60 or porphyrin core as light harvesting antennas. Synth Met 2018;245:195–201.
[40] Porcu P, Vonlanthen M, Ruiu A, González-Méndez I, Rivera E. Energy transfer in dendritic systems having pyrene peripheral groups as donors and different acceptor groups. Polymers 2018;10(10).
[41] Rojas-Montoya SM, Vonlanthen M, Porcu P, Flores-Rojas G, Ruiu A, Morales-Morales D, Rivera E. Synthesis and photophysical properties of novel pyrene-metalloporphyrin dendritic systems. Dalton Trans 2019;48(28):10435–47.
[42] Zaragoza-Galán G, Fowler MA, Duhamel J, Rein R, Solladié N, Rivera E. Synthesis and characterization of novel pyrene-dendronized porphyrins exhibiting efficient fluorescence resonance energy transfer: optical and photophysical properties. Langmuir 2012;28(30):11195–205.
[43] Zaragoza-Galán G, Fowler M, Rein R, Solladié N, Duhamel J, Rivera E. Fluorescence resonance energy transfer in partially and fully labeled pyrene

dendronized porphyrins studied with model free analysis. J Phys Chem C 2014;118 (16):8280–94.
[44] Lindsey JS, Woodford JN. A simple method for preparing magnesium porphyrins. Inorg Chem 1995;34(5):1063–9.
[45] Huang X, Groves JT. Oxygen activation and radical transformations in heme proteins and metalloporphyrins. Chem Rev 2018;118(5):2491–553.
[46] Otsuki J. Supramolecular approach towards light-harvesting materials based on porphyrins and chlorophylls. J Mater Chem 2018;6(16):6710–53.
[47] Kräutler B. Vitamin B12: chemistry and biochemistry. Biochem Soc Trans 2005;33 (4):806–10.
[48] Gouterman M. Spectra of porphyrins. J Mol Spectrosc 1961;6(C):138–63.
[49] Zheng W, Shan N, Yu L, Wang X. UV-visible, fluorescence and EPR properties of porphyrins and metalloporphyrins. Dyes Pigments 2008;77(1):153–7.
[50] Quimbym DJ, Longo FR. Luminescence studies on several tetraarylporphins and their zinc derivatives. J Am Chem Soc 1975;97(18):5111–7.
[51] Boucher LJ. Manganese porphyrin complexes. III. Spectroscopy of chloroaquo complexes of several porphyrins. J Am Chem Soc 1970;92(9):2725–30.
[52] Meunier B. Metalloporphyrins as versatile catalysts for oxidation reactions and oxidative DNA cleavage. Chem Rev 1992;92(6):1411–56.
[53] Guilard R, Kadish KM. Some aspects of organometallic chemistry in metalloporphyrin chemistry: synthesis, chemical reactivity, and electrochemical behavior of porphyrins with metal—carbon bonds. Chem Rev 1988;88(7): 1121–46.
[54] Zhang P, Hu J, Liu B, Yang J, Hou H. Recent advances in metalloporphyrins for environmental and energy applications. Chemosphere 2019;219:617–35.
[55] Araujo Pinto VH, Falcao NKSM, Mariz-Silva B, Fonseca MG, Reboucas JS. Robust Mn(III) N -pyridylporphyrin-based biomimetic catalysts for hydrocarbon oxidations: heterogenization on non-functionalized silica gel versus chloropropyl-functionalized silica gel. Dalton Trans 2020;49(45):16404–18.
[56] Gotico P, Halime Z, Aukauloo A. Recent advances in metalloporphyrin-based catalyst design towards carbon dioxide reduction: from bio-inspired second coordination sphere modifications to hierarchical architectures. Dalton Trans 2020;49(8):2381–96.
[57] Gao WY, Chrzanowski M, Ma S. Metal-metalloporphyrin frameworks: a resurging class of functional materials. Chem Soc Rev 2014;43(16):5841–66.
[58] Newkome GR, Shreiner CD. Poly(amidoamine), polypropylenimine, and related dendrimers and dendrons possessing different 1 → 2 branching motifs: an overview of the divergent procedures. Polymer 2008;49(1):1–173.
[59] Kaufman EA, Tarallo R, Elacqua E, Carberry TP, Weck M. Synthesis of well-defined bifunctional newkome-type dendrimers. Macromolecules 2017;50(13):4897–905.
[60] Kostas ID, Coutsolelos AG, Charalambidis G, Skondra A. The first use of porphyrins as catalysts in cross-coupling reactions: a water-soluble palladium complex with a porphyrin ligand as an efficient catalyst precursor for the Suzuki-Miyaura reaction in aqueous media under aerobic conditions. Tetrahedron Lett 2007;48(38): 6688–91.
[61] Newkome GR, Weis CD. Di-tert-butyl4-[(2-tert-butoxycarbonyl)ethyl]-4-aminoheptanedicarboxylate. Org Prep Proced Int 1996;28(4):495–8.
[62] Newkome GR, Moorefield CN, Baker GR, Behera RK. Cascade polymers: syntheses and characterization of one-directional arborols based on adamantane. J Org Chem 1991;56(25):7162–7.
[63] Lindsey JS, Schreiman IC, Hsu HC, Kearney PC, Marguerettaz AM. Rothemund and adler-longo reactions revisited: synthesis of tetraphenylporphyrins under equilibrium conditions. J Org Chem 1987;52(5):827–36.
[64] Lindsey JS, Wagner RW. Investigation of the synthesis of ortho-substituted tetraphenylporphyrins. J Org Chem 1989;54(4):828–36.
[65] Li F, Yang K, Tyhonas JS, MacCrum KA, Lindsey JS. Beneficial effects of salts on an acid-catalyzed condensation leading to porphyrin formation. Tetrahedron 1997;53 (37):12339–60.
[66] Kim JB, Leonard JJ, Longo FR. A mechanistic study of the synthesis and spectral properties of mero-tetraarylporphyrins. J Am Chem Soc 1972;94(11):3986–92.
[67] Lakowicz JR. Principles of fluorescence spectroscopy. third ed. New York: Springer Science; 2006.
[68] Fery-Forgues S, Lavabre D. Are fluorescence quantum yields so tricky to measure? A demonstration using familiar stationery products. J Chem Educ 1999;76(9): 1260–4.
[69] Olmsted J. Calorimetric determinations of absolute fluorescence quantum yields. J Phys Chem 1979;83(20):2581–4.